ASM Sc. J., 14, 2021

https://doi.org/10.32802/asmscj.2020.596

Window Optimisation of Power Quality Signal Detection using Gabor Transform

Muhammad Sufyan Safwan Mohamad Basir[1*], Marafa Ishaq Abdullahi[2] and Abdul Rahim Abdullah[3]

[1]*Department of Electrical Engineering, Politeknik Mukah, 96400 Mukah, Sarawak, Malaysia*

[2,4]*Faculty of Engineering and Built Environment, MAHSA University, Level 9, Engineering/Pharmacy Building, Bandar Saujana Putra, 42610 Jenjarom, Selangor, Malaysia*

[3] *Faculty of Electrical Engineering, Universiti Teknikal Malaysia Melaka, Jalan Hang Tuah Jaya, 76100 Durian Tunggal, Melaka, Malaysia*

This paper presents power quality analysis on different signal characteristics, namely instantaneous sag, momentary sag, temporary sag, instantaneous swell, momentary swell, and temporary swell. Power quality signals were analyzed using linear time-frequency distribution (TFD) namely short-time Fourier transform (STFT) and proposed Gabor transform (GT), and the best technique for power quality detection was determined based on the performance analysis of varied window length. Optimum window length for different signal characteristics which are effective and reliable for developing real-time monitoring system was employed using MATLAB. From a time-frequency representation (TFR) results based on STFT and GT, parameters such as instantaneous RMS voltage, $V_{RMS}(t)$ and instantaneous total waveform distortion, $V_{TWD}(t)$ had been extracted. In finding the best technique for power quality, the TFDs had been compared in terms of accuracy, memory and computational complexity of the analysis. Based on the performance analysis conducted, GT was able to compute with high accuracy with 94% averagely as well as low memory size by 6% compared to STFT. Hence, GT is considered as the best TFD, and recommended for low cost PQ monitoring system.

Keywords: power quality; sag; swell; Gabor transform

I. INTRODUCTION

Power Quality (PQ) issues are of main concern nowadays in electrical and electronics materials since the impact can cause losses to sensitive equipment, in accordance with wide implementation of power electronics components. Institute of Electrical and Electronic Engineers (IEEE) Standard, IEEE 1100-2015 defines PQ as "the concept of powering and ground the sensitive electronic instrument in a way suitable for the equipment" (Sivakumar *et al.,* 2016). PQ comprises of the quality of voltage, quality of current and capability to maintain a sinusoidal waveform at rated voltage and frequency (Sankaran, 2001). PQ is classified into three, i.e. waveform distortion (harmonic and interharmonic), variation of voltage (instantaneous sag, momentary sag, temporary sag, instantaneous swell, momentary swell and temporary swell), and transient signal (Szmajda *et al.,* 2010). Fluctuation in signal amplitude, phase and frequency in power system, e.g. a sensitive power system, will cause a sudden increase or decrease (sag and swell) in network signal, as well as high amplitude in high frequency components (transient).

In engineering field, determining the types of signal is quite difficult since signal behaviours may be different (Styvaktakis *et al.,* 2001). Conceptually, distortion in current, voltage and frequency outcomes from PQ can be monitored by using certain techniques like frequency distribution and time-frequency distribution (TFD) (Muhamad *et al.,* 2007). PQ analyzer is commonly used to

*Corresponding author's e-mail: sufyan@pmu.edu.my

detect the behaviour of waveform by comparing voltage readings between two accurate voltmeters measuring the same system voltage. IEEE power quality standards 419-2014 and national fire protection system (NFPA) 70B are excellent resources to help understand PQ terminology, issues and corrective actions (Yusoff *et. al.,* 2017; Sakthivel *et al.,* 2003).

The use of signal processing technique for PQ provides meaningful and valuable information on current and voltage signals. The analyzed signal can be presented in frequency and time domain. Measurement of PQ parameters are performed with the help of fast Fourier transform (FFT) (Ribeiro *et al.,* 2007). The disadvantage of this technique is that, it cannot provide accurate information when there is a change in spectrum, given that the analyzed signal is only presented in frequency domain. Hence, time frequency distribution is introduced to overcome time varying issue. This technique can be divided into two categories, which are linear methods (linear window), which include short-time Fourier transform (STFT), Gabor transform (GT) and wavelet transform (WT), and bilinear methods (cross term window) such as Wigner-Ville distribution (WVD), Pseudo Wigner-Ville distribution (PWVD), smoothed Pseudo Wigner-Ville distribution, and Choi-Williams distribution (CWD) (Janiszewski, 2012; Satish, 1998; Tarasiuk, 2007). The aim of this paper is to benchmark the proposed GT with STFT in term of accuracy of measurement, computational complexity and memory. The outcome of the proposed technique should able to compromise with all these performances. Hence future work for a real-time monitoring system can be developed.

II. TYPES OF POWER QUALITY

PQ disturbance is classified into five, which are sag, swell, undervoltage, overvoltage and transient. All these types are generally categorized according to their various time and magnitude (see Table 1) (Ekici, 2009). Undervoltage and overvoltage events are named due to their duration and magnitude. Overvoltage events of a very short time and a high magnitude are referred to as transient overvoltage (Bollen, 2000). Distinctively, overvoltage over half of cycle duration is different from the short duration overvoltage.

Table 1. Categories and classification of electromagnetic phenomena in power system according to IEEE-1159 standard

Categories	Power Quality	Duration	Magnitude
Transient	Impulsive	< 50 ns	0 – 4 pu
	• Nanosecond	50 ns – 1 ms	
	• Microsecond Oscillatory	1 ms	
	• Low frequency	0.1ms – 50 ms	0 – 8 pu
		20 μs	
Short duration variation	Instantaneous		
	• Sag	0.5 – 30 cycles	1.1 – 0.9 pu
	• Swell	0.5 – 30 cycles	1.1 – 1.8 pu
	Momentary		
	• Sag	30 cycles – 3s	1.1 – 0.9 pu
	• Swell	30 cycles – 3s	1.1 – 1.4 pu
	Temporary		
	• Sag	3s – 1 min	1.1 – 0.9 pu
	• Swell	3s – 1 min	1.1 – 1.2 pu
Long duration variation	Undervoltage	>1 min	0.2 – 0.9 pu
	Overvoltage	>1 min	1.1 – 1.3 pu

III. TIME FREQUENCY DISTRIBUTION

Time varying signal is commonly analyzed using TFDs. With the use of TFD, variables *t* and *f,* which are presented in three-dimensional are known as time-frequency representation (TFR) but not exclusively mutual. Variable *t* cross-section describes the time, and variable *f* describes the present frequency (Boashash, 2015). Therefore, signal

analysis using TFD promises high accuracy system, and low in memory size for estimations. Linear TFD such as STFT and GT are shown in Table 2.

A. Short-Time Fourier Transform

STFT that works with window is able to detect fluctuation, but the selection of window length must be optimised because high rates of fluctuation will give rise to significant error (Santoso *et al.,* 2000). Unlike FT, STFT takes into account the changes of time in signal spectrum. Time and frequency resolutions of product are constant, and it is fundamental limitation of the STFT technique (Poisson *et al.,* 1999). The PQ that took place within a short amount of time (within 11.2 ms) can be detected using STFT. Previous experiments proved that WT is superior compared to STFT (Mahela *et al.,* 2015). Analysis based on whale click showed that the STFT cannot resist noise compared to WT, but the problem can be sorted by setting a suitable threshold value for reduction of noise (Lopatka *et al.,* 2005). However, STFT is still the preferred choice due to its low complexity, which is suitable for real-time monitoring system.

B. Gabor Transform

GT is a next-level version of STFT, in which the signal of the input is time-nominated by a window function (Gaussian window), and transformed by FT to conduct the time frequency analysis (Cho *et al.,* 2009). Discrete Gabor transform (DGT) is similar to STFT, except that it uses a Gaussian window. For a periodic sequence and finite, it can be expanded as a linear combination of the Gabor coefficient and the basic functions (Granados-Lieberman *et al.,* 2011). Like STFT, the GT has a demerit of compromise between time and frequency resolution, that is caused by the width of the window. A long window gives a good frequency resolution but poor time resolutions. As the window size becomes broader, the frequency resolution becomes worse, but the time resolution improves (Basir *et al.,* 2019).

Table 2. Specification for signal processing method

Methods	Equation	Window
STFT	$S_x(t,f)=\int_{-\infty}^{\infty} x(\tau-1)w(\tau-1)e^{-j2\pi\tau}d\tau$	Hanning
GT	$C(n,k)=\int_{-\infty}^{\infty} x(\tau)w(\tau-nT_w)e^{-j2f_0\tau}d\tau$	Gaussian

IV. SIGNAL MODELLING

Different PQ disturbance embodies different signal characteristics. In this research, six types of PQ disturbance, namely instantaneous sag, momentary sag, temporary sag, instantaneous swell, momentary swell, and temporary swell, were studied. PQ signals were generated using MATLAB. According to IEEE standard 1159-2009, the equation can be derived using a complex exponential function as tabulated in Table 3. During the signal testing, parameters such as starting time, t amplitude, A duration, (t-tk-1) and frequency, f can be temporarily chosen and changed depending on the outcome desired. Technically, A_1 and f_o were 1 and 50Hz (fundamental frequency), respectively, while the sampling frequency, fs was set to 12000Hz with 6000Hz as the approximate maximum frequency components.

Table 3. Characteristic of power quality signals

Power quality	Equations	Signals Components
Normal	$X_{norm}(t)=Ae^{j2t}$	A=1
Instantaneous Sag	$X_{vv}(t)=A_{1,3}e^{2\pi f_0 t}\sum_{k=1}^{k}A_2k\prod k(t-t_{k-1})$	A_1=A_3=1, A_2=0.5, t_1=100 ms, t_2=150 ms
Momentary Sag		A_1=A_3=1, A_2=0.5, t_1=100 ms, t_2=600 ms
Temporary Sag		A_1=A_3=1, A_2=0.5, t_1=100 ms, t_2=3100 ms
Instantaneous Swell		A_1=A_3=1, A_2=1.8, t_1=200 ms, t_2=250 ms
Momentary Swell		A_1=A_3=1, A_2=1.4, t_1=200 ms, t_2=700 ms
Temporary Swell		A_1=A_3=1, A_2=1.2, t_1=200 ms, t_2=3200 ms

As shown in Table 3, the x_{norm} was modelled with the amplitude A=1 with duration, $t_{duration}$ of $(1/F_s) \times N_s$ but this was not regarded to PQ. Using STFT might result in dropping of time or frequency when analyzing the signal;

thus it was preferable to capture the optimum window in order to avoid inaccuracy in the measurements. PQ signals such as instantaneous sag, momentary sag and temporary sag with A_2=0.5 and instantaneous swell with A_2=1.8, momentary swell with A_2=1.4 and temporary swell with A_2=1.2 were chosen, in finding the suitable optimum window size in order to give merits in real-time monitoring system.

A. Instantaneous Sag

Figure 1(a) displays the signal disturbance of 50 ms cover four cycles with magnitude of 0.5 pu. Figure 1(b) shows TFR using GT to identify the characteristics of the signal, where the disturbance appeared for 50 ms and the magnitude is reduced from 1 to 0.5 pu. The parameters of sag signal were estimated from TFR to identify the characteristics of the signal. Figure 1(c) shows that the instantaneous RMS voltage decreased from 1 to 0.5 pu, starting at 50 ms for a duration of 50 ms. Figure 1(d) shows that the magnitude of instantaneous total waveform distortion increased from 0 to 10% for a duration of 50 ms during the instantaneous sag phenomena.

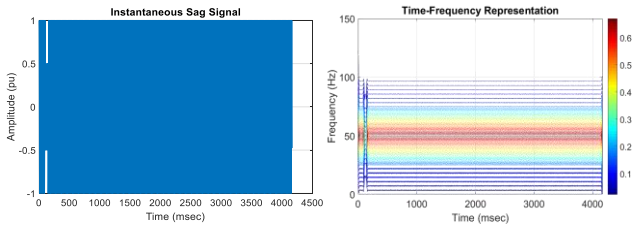

(a) (b)

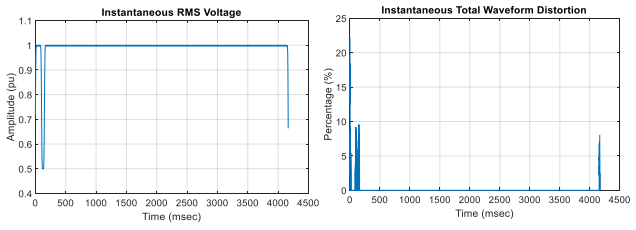

(c) (d)

Figure 1. Power quality signal for, (a) instantaneous sag and its, (b) TFR using GT, (c) instantaneous RMS voltage, $V_{RMS}(t)$, (d) instantaneous total waveform distortion, $V_{TWD}(t)$

B. Momentary Sag

Figure 2(a) shows the momentary sag signal using GT with a magnitude of 0.5 pu, which lasted for 500 ms. Figure 2(b) shows that TFR results from GT to identify the characteristics of the signal, where the disturbance appeared for 500 ms and cause the magnitude to drop from 1 to 0.5 pu. Since the magnitude of sag disturbance is lower than normal signal, TFR that indicates by blue stripe represent the disturbance, while dark red stripe shows the normal signal. Figure 2(c) shows similar trend to previous instantaneous sag, by means the RMS voltage decreased by 0.5 pu for a duration of 500 ms. Figure 2(d) shows that the total waveform distortion indicated by 0% for the whole signal cycles.

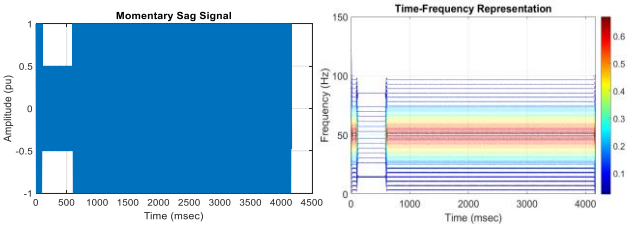

(a) (b)

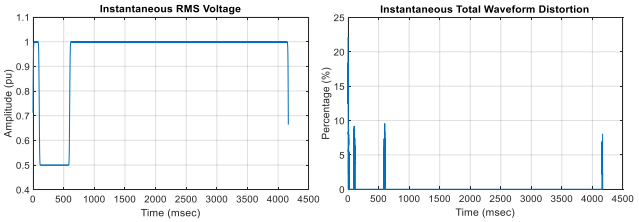

(c) (d)

Figure 2. Power quality signal for, (a) momentary sag and its, (b) TFR using GT, (c) instantaneous RMS voltage, $V_{RMS}(t)$, (d) instantaneous total waveform distortion, $V_{TWD}(t)$

C. Temporary Sag

The difference of temporary sag is the signal lasted for more than 3 s and for this case, disturbance is modelled for 3000 ms with magnitude of 0.5 p.u (see Figure 3(a)). Also similar to previous sag characteristics, the RMS voltage as shown in Figure 3(c) decreased by 0.5 pu for a duration of 3000 ms. Figure 3(d) shows the total waveform distortion indicated a noise during the initial process of transition from normal signal to disturbance signal with an increment of 10%. This spark of noise also occurs when there is a transition between disturbance signal to normal signal due to the use of window function that have a sharp transition which gives a poor frequency localization and cannot be avoided unless we threshold the STFT.

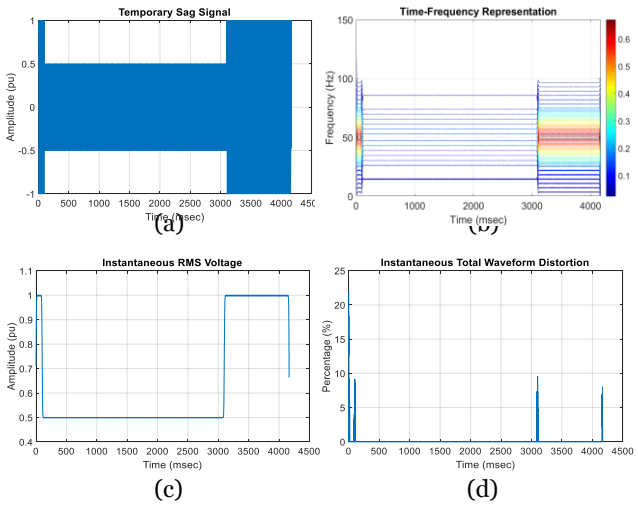

Figure 3. Power quality signal for, (a) temporary sag and its, (b) TFR using GT, (c) instantaneous RMS voltage, $V_{RMS}(t)$, (d) instantaneous total waveform distortion, $V_{TWD}(t)$

D. Instantaneous Swell

Figure 4(a) shows that the magnitude of the power quality of instantaneous swell signal increased from 1 to 1.8 pu for a duration of 50 ms. The duration for the instantaneous swell signal is similar to previous instantaneous sag but with the increased magnitude of 0.8 p.u of a normal signal. As shown in Figure 4(c), the instantaneous RMS voltage increased from 1 to 1.8 pu, starting from 200 ms for a duration of 50 ms. Figure 4(d) shows that the magnitude of the instantaneous total wave distortion increased from 0 to 10% during the initial stage of transition from normal signal to disturbance signal and is lasted for around 10 ms results from GT as in Figure 4(b). The selection of 12000 Hz of sampling frequency contributes to measurement of frequency up to 6000 Hz. For this case, the swell signal modelled adapts similar frequency as normal signal cause the magnitude of TFR appears at 50 Hz.

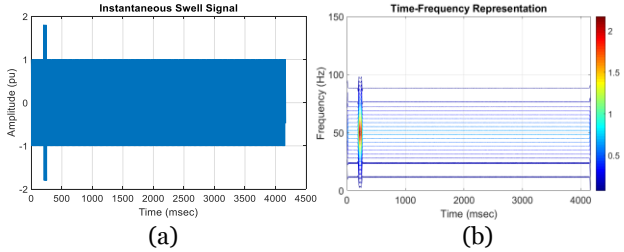

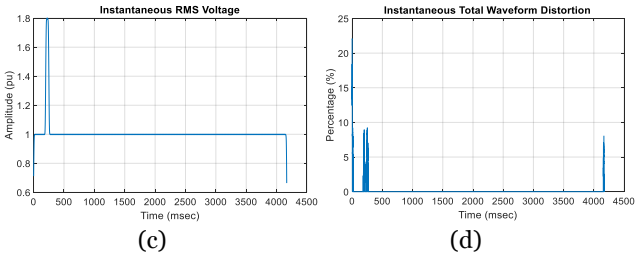

Figure 4. Power quality signal for, (a) instantaneous swell and its, (b) TFR using GT, (c) instantaneous RMS voltage, $V_{RMS}(t)$, (d) instantaneous total waveform distortion, $V_{TWD}(t)$

E. Momentary Swell

Figure 5(a) shows that the magnitude of the power quality of momentary swell signal increased from 1 to 1.8 pu for a duration of 500 ms. Figure 5(b) shows TFR and signal of momentary swell estimated from the TFR using GT. The blue strip lines indicate normal signal, while the dark red stripe indicates the swell characteristics of the analysis. As shown in Figure 5(c), the instantaneous RMS voltage increased from 1 to 1.8 pu, starting from 200 ms for a duration 500 ms.

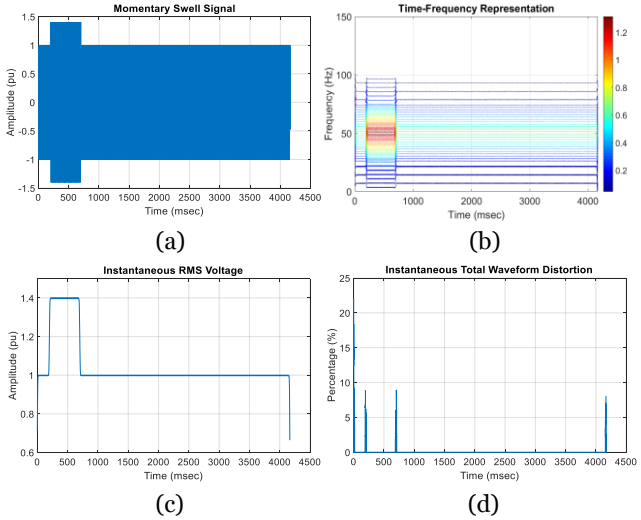

Figure 5 . Power quality signal for, (a) momentary swell and its, (b) TFR using GT, (c) instantaneous RMS voltage, $V_{RMS}(t)$, (d) instantaneous total waveform distortion, $V_{TWD}(t)$

F. Temporary Swell

As shown in Figure 6(a), the magnitude of the temporary swell signal increased from 1 to 1.8 pu. By following the IEEE standard-1159 as illustrated in Table 1, the condition for temporary swell duration should last more than 3 s is followed. The trend for TFR (Figure 6(b)) and parameters for temporary swell signal is quite similar to temporary sag signal, but with different magnitude, by means normal signal magnitude is lower than swell signal.

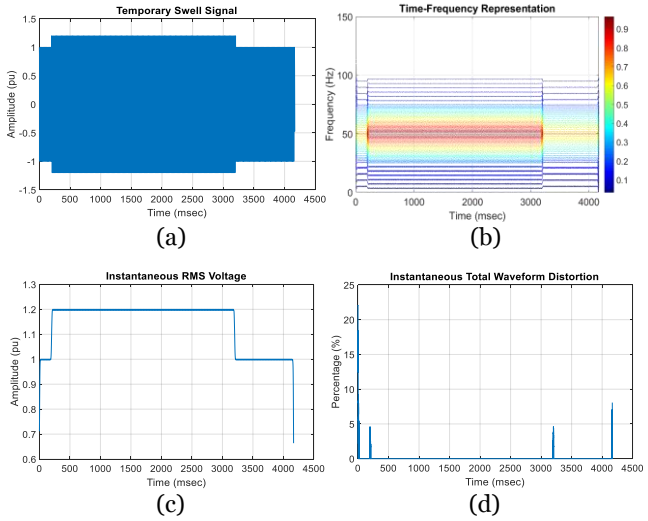

Figure 6. Power quality signal for, (a) temporary swell and its, (b) TFR using GT, (c) instantaneous RMS voltage, $V_{RMS}(t)$, (d) instantaneous total waveform distortion, $V_{TWD}(t)$

V. TIME FREQUENCY DISTRIBUTION PERFORMANCE ANALYSIS

In effort to determine the best technique among all linear time-frequency distribution, it is important to compare their TFDs in terms of accuracy of the analysis, memory size of the analysis and computational complexity of the analysis.

A. Accuracy of The Analysis

In this study, the mean absolute percentage error (MAPE) values of instantaneous sag, momentary sag, temporary sag, instantaneous swell, momentary swell and temporary swell had been computed for ten different signals in order to obtain the average percentage error for the accuracy of TFDs which are shown in Figure 7 and Figure 8. The MAPE was computed using Equation (1). Actual value, A_1 and measured value, F_1 had been tested by the number of data, n.

$$MAPE = \frac{100\%}{n}\sum_{t-1}^{n}\left|\frac{A_t - F_t}{A_t}\right| \quad (1)$$

The optimum window length obtained from STFT using MAPE and the proposed GT is compared. The sag signals modelled consists of instantaneous, momentary and temporary were simulated with 10 different signals with various characteristics for each type of PQ signals. The graph in Figure 7 indicates an unreasonable error in window length of 128 for both techniques. The graph trend shows a decrement in MAPE when the window length is increased. In instantaneous sag, momentary sag and temporary sag accuracy of the analysis show that the MAPE of the Gabor Transform with window length of 480 was averagely 0.6% lower than STFT simulated with 512. This means GT can provide more accurate results than STFT. Besides, increases the window length from 512 to 1024 either STFT or GT will not guarantee the decrement in MAPE where the outcome shows this technique suffers for additional 18% error, and this case is for instantaneous sag.

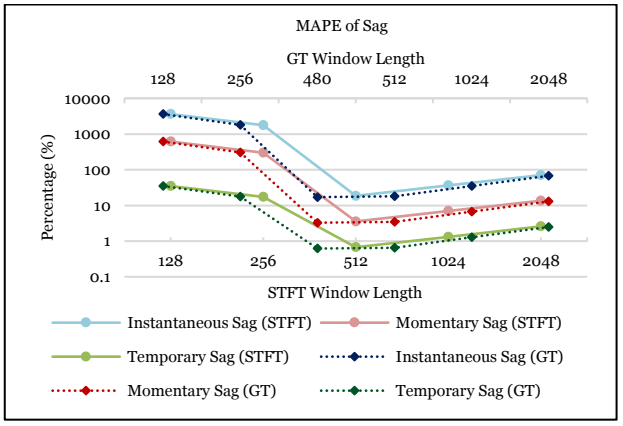

Figure 7. MAPE of sag analysis for STFT and GT

The effect of window length in time and frequency marginals are intuitively investigated. The corrupted swell signal modelled is simulated with varied window length (128 to 2048) for the purpose of reliability of the measurement. As can be seen in Figure 8, the lowest MAPE is 0.03% indicated by GT with window length of 480 at temporary swell signal. Although the selected 480 window length is considered the best, the outcomes show this method is unable to perform well for instantaneous swell. The window length of 256 indicated lower error by 9%. In addition, the error indicated by STFT is larger compared to GT for all

three cases, hence the optimum point of the 480 using GT is an appropriate choice.

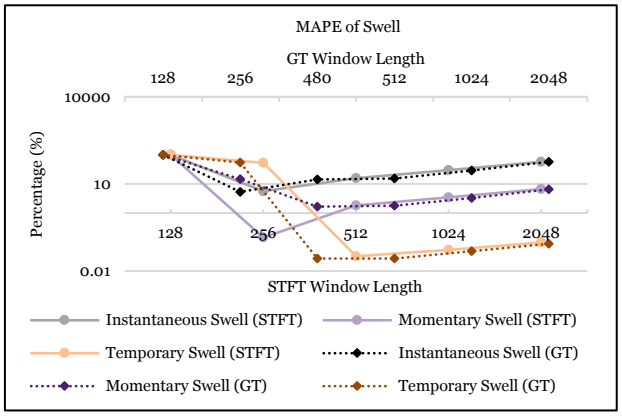

Figure 8. MAPE of swell analysis for STFT and GT

B. Computational Complexity of The Analysis

Figure 9 shows the graph of computational complexity analysis of the window length of the modelled signals using Equations (2) and (3). The TFDs which are STFT and GT complexity depended on the window length and the number of samples, N_s was chosen for the analysis for all the PQ signals which were the same for both TFDs. Different TFD would give different categories of complexity in which the frequency would affect the window length. Computational complexity has two variables which are the signal length, N and the window length, N_w.

$$Cr_{STFT} = N - N_w\left(N_w \log_2\left(N_w\right)\right) \tag{2}$$

$$Cr_{GT} = N - N_w\left(N_w^{\,2}\right) \tag{3}$$

Based on Equation (3), STFT that employ fast Fourier transform (FFT) offers fast computation compared to GT which performs discrete Fourier transform (DFT). The computation of DFT requires N^2 complex multiplications but FFT reduces the DFT computation to $(N/2)\log_2(N)$ complex multiplication. Besides, higher number of frequency component may contribute to computation complexity, and for PQ cases should be measured up to 50th components. Instead, for a signal in time domain, there are values along the time axis and all samples need to be considered to contribute much computation to calculate the TFR.

The lowest window length may benefit in low complexity; however, the reliability of measurement related to accuracy should also be considered. A graph in Figure 9 illustrates GT is more complex compared to STFT although the measurement of accuracy is much more superior. The complexity of GT with 480 is double compared to STFT with 512. GT complexity is still considered low, under the circumstance that other TFD such as continuous WT or Hilbert-Huang transform is unsuited for real-time monitoring system (Bouchikhi *et al.*, 2011).

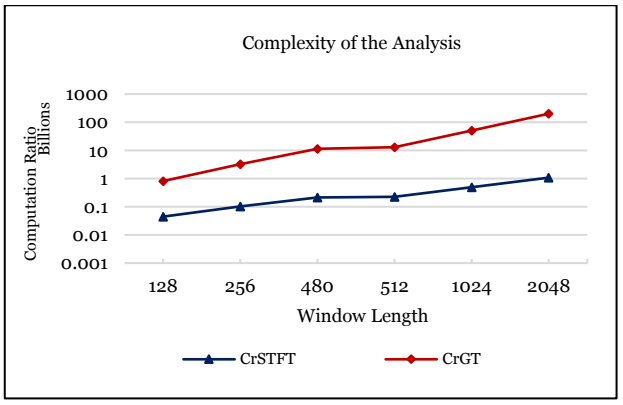

Figure 9. Computational complexity for STFT and GT

C. Memory Size of The Analysis

With the use of the same equation, both STFT and GT techniques share similar memory for any varies window (see Figure 10). The values only differ in terms of the window length used in the analysis. The graph clearly shows that GT with 480 window length provided slightly lower memory size compared to STFT 512 window length. Similar to computational complexity, the memory selected should compromise with the accuracy of the measurements, hence 2764800 Mbyte of memory is required for PQ measurement.

$$Memory_{LinearTFD} = \frac{N_w\left(N - N_w\right)}{N_s} \tag{4}$$

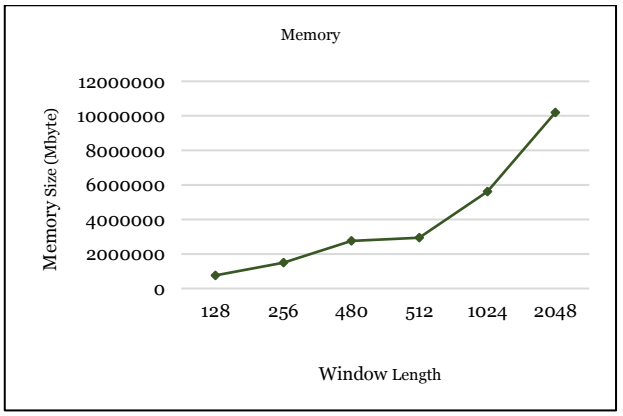

Figure 10. Memory size for STFT and GT

VI. BEST TECHNIQUE

The outcomes of the PQ signals for both TFDs had been compared in terms of accuracy, computational complexity and memory of the analysis and plotted on a bar graph, as shown in Figure 11. In order to determine the best TFD in the comparison process, the optimum window length for STFT with 512 and GT with 480 is chosen. It should be considered that accuracy becomes the highest priority in selecting the best TFD that gives reliability in real-time monitoring system to produce an accurate result. The second in command is the computational complexity that plays a role in providing the signal parameters either in short or long duration of time. The last aspect is considerable in memory size that can affect the cost and the size of the system as high memory size requires high memory space and better processor performance.

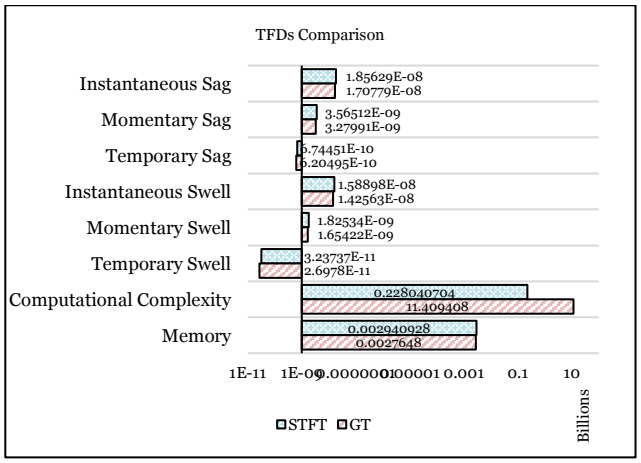

Figure 11. The comparison of the STFT and GT based on accuracy, computational complexity and memory size of the analysis

The comparison based on accuracy shows that GT able to surpass STFT with a slightly different percentage error for all the PQ signals. However, this technique suffers from additional computational complexity results from DFT computation which lead to slow in estimating the parameters. In addition, the memory requires for both GT is 6% lower than STFT. The STFT gave a higher percentage error and memory size of the analysis with low computational complexity of the analysis, which is undesirable, but lower memory is actually better for the system. Therefore, by considering the reliability of the measurement, GT with 480 window length is selected as the best TFD for a PQ analysis. For a further PQ analysis that relates to real-time monitoring system, GT should be considered since the use of Gaussian window can improve the system accuracy (Jopri *et al.,* 2017).

VII. CONCLUSION

The TFDs performance in the PQ analysis using STFT and GT had been compared in terms of accuracy of the analysis, memory size and computational complexity of the analysis. The PQ signals had been modelled follow IEEE standard-1159 and the analysis is conducted using MATLAB. The window length is varied in finding the optimum value that can negotiate with the TFD performance. The comparison between STFT and GT with selected window length of 512 and 480, respectively shows GT gave low MAPE and memory size of the analysis than STFT. It is recommended to employ GT for PQ analysis in developing a low-cost monitoring system.

VIII. ACKNOWLEDGEMENT

The authors would like to thanks Department of Electrical Engineering, Politeknik Mukah Sarawak, Ministry of Higher Education Malaysia and School of Microelectronic Engineering, Universiti Malaysia Perlis for providing the support for this research. Thank you in advance for the cooperation provided by MAHSA University and Universiti Teknikal Malaysia Melaka.

IX. REFERENCES

Abdullah, AR, Sha'ameri, AZ, Sidek, ARM & Shaari, MR 2007, 'Detection and classification of power quality disturbances using time-frequency analysis technique', in 2007 5th Student Conference on Research and Development, IEEE, pp. 1-6.

Basir, MSSM, Abdullah, AR & Saad, NM 2019, 'A

comparative study on spectrogram and S-transform for batteries parameters estimation', Jurnal Teknologi, vol. 81, no. 2.

Boashash, B 2015, Time-frequency signal analysis and processing: a comprehensive reference, 2nd edn, Academic Press, US.

Bollen, MH 2000, 'Understanding power quality problems', in Voltage sags and Interruptions. IEEE press.

Bouchikhi, EH, Choqueuse, V, Benbouzid, MEH, Charpentier, JF & Barakat, G 2011, 'A comparative study of time-frequency representations for fault detection in wind turbine', in IECON 2011-37th Annual Conference of the IEEE Industrial Electronics Society, IEEE, pp. 3584-3589.

Carlsson, F, Engström, J & Sadarangani, C 2001, 'Simulations of a synchronous machine affected by voltage sags. mH, vol. 17, no. 50, pp. 37-0.

Cho, SH, Jang, G & Kwon, SH 2009, 'Time-frequency analysis of power-quality disturbances via the Gabor–Wigner transform', IEEE Transactions on Power Delivery, vol. 25, no. 1, pp. 494-499.

Ekici, S 2009, 'Classification of power system disturbances using support vector machines', Expert Systems with Applications, vol. 36, no. 6, pp. 9859-9868.

Fitzer, C, Barnes, M & Green, P 2004, 'Voltage sag detection technique for a dynamic voltage restorer', IEEE Transactions on Industry Applications, vol. 40, no. 1, pp. 203-212.

Fuchs, E & Masoum, MA 2011, Power quality in power systems and electrical machines, 2nd edn, Academic press, US.

Granados-Lieberman, D, Romero-Troncoso, RJ, Osornio-Rios, RA, Garcia-Perez, A & Cabal-Yepez, E 2011, 'Techniques and methodologies for power quality analysis and disturbances classification in power systems: a review', IET Generation, Transmission & Distribution, vol. 5, no. 4, pp. 519-529.

Haichun, L, Lizhi, X & Shaojun, X 2009, 'A new detection method of voltage sag based on period phase concept', in 2009 4th IEEE Conference on Industrial Electronics and Applications, IEEE, pp. 3333-3337.

Janiszewski, J 2012, 'Measurement procedure of ring motion with the use of highspeed camera during electromagnetic expansion', Metrology and Measurement Systems, vol. 19, no. 4, pp. 797-804.

Jopri, MH, Abdullah, AR, Sutikno, T, Manap, M & Yusoff, MR 2017, 'A utilisation of improved Gabor transform for harmonic signals detection and classification analysis', International Journal of Electrical and Computer Engineering, vol. 7, no. 1, pp. 21.

Lopatka, M, Adam, O, Laplanche, C, Zarzycki, J & Motsch, JF 2005, 'An attractive alternative for sperm whale click detection using the wavelet transform in comparison to the Fourier spectrogram', Aquatic Mammals, vol. 31, no. 4, pp. 463-467.

Mahela, OP, Shaik, AG & Gupta, N 2015, 'A critical review of detection and classification of power quality events', Renewable and Sustainable Energy Reviews, vol. 41, pp. 495-505.

Muhamad, MI, Mariun, N & Radzi, MAM 2007, 'The effects of power quality to the industries', in 2007 5th Student Conference on Research and Development, IEEE, pp. 1-4.

Poisson, O, Rioual, P & Meunier, M 1999, 'New signal processing tools applied to power quality analysis', IEEE Transactions on Power Delivery, vol. 14, no. 2, pp. 561-566.

Ribeiro, MV, Szczupak, J, Iravani, MR, Gu, IY, Dash, PK & Mamishev, AV 2007, 'Emerging signal processing techniques for power quality applications', EURASIP Journal of Advances in Signal Processing.

Sakthivel, KN, Das, SK & Kini, KR 2003, 'Importance of quality AC power distribution and understanding of EMC standards IEC 61000-3-2, IEC 61000-3-3 and IEC 61000-3-11', in 8th International Conference on Electromagnetic Interference and Compatibility, IEEE, pp. 423-430.

Sankaran, C 2017, Power quality. CRC Press, US.

Santoso, S, Grady, WM, Powers, EJ, Lamoree, J & Bhatt, SC 2000, 'Characterization of distribution power quality events with Fourier and wavelet transforms', IEEE Transactions on Power Delivery, vol. 15, no. 1, pp. 247-254.

Satish, L 1998, 'Short-time Fourier and wavelet transforms for fault detection in power transformers during impulse tests', IEE Proceedings-Science, Measurement and Technology, vol. 145, no. 2, pp. 77-84.

Sivakumar, D, Srividhya, JP & Shanmathi, T 2016, 'A review on power quality monitoring and its controlling techniques', in 8th International Conference on Latest Trends in Engineering and Technology (ICLTET'2016) 5-6 May 2016, Dubai, UAE, pp. 5-6.

Styvaktakis, E, Gu, IY & Bollen, MH 2001, 'Voltage dip

detection and power system transients', in 2001 Power Engineering Society Summer Meeting, Conference Proceedings (Cat. No. 01CH37262), IEEE, vol. 1, pp. 683-688.

Szmajda, M, Górecki, K & Mroczka, J 2010, 'Gabor transform, Gabor-Wigner transform and SPWVD as a time-frequency analysis of power quality', in Proceedings of 14th International Conference on Harmonics and Quality of Power-ICHQP September 2010, IEEE, pp. 1-8.

Tarasiuk, T 2006, 'Hybrid wavelet–Fourier method for harmonics and harmonic subgroups measurement—Case study', IEEE Transactions on Power Delivery, vol. 22, no. 1, pp. 4-17.

Yusoff, MR, Jopri, MH, Abdullah, AR, Sutikno, T, Manap, M & Hussin, AS 2017, 'An analysis of harmonic and interharmonic contribution of electric arc furnace by using periodogram', International Journal of Electrical and Computer Engineering, vol. 7, no. 6, pp. 3753.